POLITECNICO DI TORINO
Repository ISTITUZIONALE

Characterization and Finite Element Analyses of Tensile and Bending Behavior of Nylon Reinforced with Continuous Carbon Fiber Produced by Additive Manufacturing

Original
Characterization and Finite Element Analyses of Tensile and Bending Behavior of Nylon Reinforced with Continuous Carbon Fiber Produced by Additive Manufacturing / Galati, M., Minetola, P., Rizza, G.. - In: JOURNAL OF MATERIALS ENGINEERING AND PERFORMANCE. - ISSN 1544-1024. - ELETTRONICO. - (2025). [10.1007/s11665-025-11934-8]

Availability:
This version is available at: 11583/3003146 since: 2025-09-18T15:08:17Z

Publisher:
SPRINGER

Published
DOI:10.1007/s11665-025-11934-8

Terms of use:

This article is made available under terms and conditions as specified in the corresponding bibliographic description in the repository

Publisher copyright

(Article begins on next page)

18 November 2026

JMEPEG
https://doi.org/10.1007/s11665-025-11934-8

©The Author(s)
1059-9495/$19.00

ORIGINAL RESEARCH ARTICLE

Characterization and Finite Element Analyses of Tensile and Bending Behavior of Nylon Reinforced with Continuous Carbon Fiber Produced by Additive Manufacturing

Manuela Galati, Paolo Minetola, and Giovanni Rizza

Submitted: 7 November 2024 / Revised: 21 January 2025 / Accepted: 21 June 2025

Leveraging advancements in extrusion technology, continuous filament fabrication (CFF) offers a cutting-edge approach to producing composite components layer by layer. What sets this technique apart is its ability to apply reinforcements precisely where needed, optimizing both performance and sustainability. The adopted approach to depositing the fiber using a reinforced filament is critical in determining the final characteristics. Despite its potential, there is limited understanding of mechanical performance, particularly under bending conditions and when only a few reinforced layers are used. This study investigates the mechanical behavior of CFF-produced composite materials under tensile and bending loads. Reinforced samples were fabricated and tested under varying conditions, such as fiber orientation, number of reinforcement layers, and placement along the build direction. The localized reinforcement capability of CFF highlights the importance of numerical modeling in virtually testing structures before production. To this end, the experimental results were replicated in a numerical environment, enabling precise calibration of a finite element model to predict the mechanical behavior of reinforced components.

Keywords CFF, FE analysis, fiber-reinforced material, mechanical characterization

1. Introduction

Over the years, the applications of additive manufacturing (AM) have been growing to a great extent (Ref 1, 2). These production techniques rely on creating components layer by layer that have particular applications in the field of medical treatments (Ref 3, 4), aerospace (Ref 5, 6), and automotive (Ref 7). Initially, AM evolved toward the use of a single material for the final product, while the possibility of using an additional material was exclusively destined as a secondary material for supporting the component construction. However, the possibility opened by the local control offered by AM has allowed the production of functionalized components using simultaneously different materials with different properties. The industrial applications of these techniques are rapidly growing (Ref 8, 9), particularly in the production of small components in limited series (down to a single part) such as aerodynamic components with high specific strength and rigidity (Ref 9) or components with controlled energy absorption through the manufacturing process design (Ref 8). In such cases, where molds are costly, composites can replace metallic components, offering significant advantages in terms of weight reduction and sustainability. This is the case of continuous filament fabrication (CFF), patented by Markforged, a revolutionary technology based on material extrusion in which an additional nozzle in a material extrusion system is used to deposit a reinforcement fiber in a continuous manner. Contrary to the conventional manufacturing process for reinforced components, CFF allows the deposition of the reinforcing fiber in localized areas where only it is needed (Ref 10). This approach introduces a new class of components where the use of reinforcing fibers is optimized for efficiency. Components produced using CFF can be designed not only to enhance the orientation and deposition of the reinforced layers but also to minimize fiber usage, potentially creating matrix-dominant materials. This innovation significantly improves the recyclability of the composites, addressing a critical challenge posed by the presence of multiple constituents in traditional composite materials. By incorporating minimal fiber reinforcement, it becomes possible to develop lightweight, durable, and environmentally friendly composites, expanding their applicability to areas previously unexplored, such as wearable devices.

In contrast to the conventional fiber distribution, which is controlled solely by the orientation angle, with CFF, new fiber distribution patterns can be achieved, leading to composite materials with enhanced or novel properties. For example, Melenka et al. (Ref 11) showed an increase in stiffness and ultimate strength of the test samples in which the Kevlar fiber was deposited with concentric rings. Van Der Klift et al. (Ref 12) showed that the deposition of carbon fiber significantly improved the mechanical properties of the matrix, commonly

Manuela Galati, Paolo Minetola, and **Giovanni Rizza**, Department of Management and Production Engineering (DIGEP), Integrated Additive Manufacturing center (IAM@PoliTo), Politecnico di Torino, Corso Duca degli Abruzzi 24, 10129 Torino, Italy. Contact e-mail: giovanni.rizza@polito.it.

Published online: 02 September 2025

nylon-based. Islam et al. (Ref 13) demonstrated a greater capacity for energy dissipation for nylon reinforced with carbon fiber manufactured using AM methods, in contrast to injection-molded nylon. Dickson et al. (Ref 14) studied the mechanical tensile performances of continuous carbon, Kevlar, and glass fiber-reinforced nylon composites according to the possibility of controlling the fiber orientation and the percentage of the infill density. However, Justo et al. (Ref 15) proved that the properties of 3D-printed nylon reinforced with carbon or fiberglass with the same angle of pre-pregs obtained by traditional methods are lower. Similar research is conducted to exploit the potential of AM to use reinforcement in a reinforced matrix with short fiber. A commercial example of such a matrix is a carbon microfiber-reinforced nylon, named Onyx, which can be used as a matrix filament in the CFF process or directly as reinforced material in parts that cannot be filled with reinforcement (Ref 16). The microfiber contained in Onyx makes it much stronger and stiffer compared to the pure thermoplastic nylon matrix. However, composite reinforced with short or microfiber presents significant challenges during recycling. This makes the use of AM for composites reinforced with long fibers more aligned with sustainable practices and circular economy goals compared to those with short or microfibers (Ref 17).

However, most of the scientific research which focuses on the application of a pure nylon matrix and a low fiber volume ratio is at an early stage and mainly focused on an empirical analysis of the effect of the processing technology on mechanical properties. In this context, most of the testing experiments were performed under tensile or compression loads (Ref 18) and are limited to the investigation of a few configurations of parameters and high content of fibers. The reinforcement pattern, the path distribution, the print orientation, and the percentage of fiber are the parameters that affect the mechanical properties the most (Ref 19). On the other hand, it appeared that the layer thickness has a marginal effect over the other factors (Ref 20). Since the materials differ significantly from conventional composites, predicting the properties of this new class of components, despite insights from experimental data, is essential for effectively linking the manufacturing process to product design (Ref 21). This aspect is more important when selecting specific areas for the reinforcement or predicting the properties of complex components. As far as the tensile properties are concerned, Galati et al. (Ref 22) developed a methodological approach for modeling the three-dimensional properties of a reinforced material printed using the CFF process. The analysis was implemented on a finite element (FE) model and validated for different fiber orientations but using only a single reinforced layer. However, this condition is limiting because the current use of the technology, and more in general reinforced components, involves sandwich structures. Additionally, the model was calibrated using an out-of-production material, recently replaced by Markforged with the so-called nylon white to improve material integrity.

This work extends the findings of Galati et al. (Ref 22) to the use of the new nylon matrix material (called commercially, nylon white) for low carbon fiber volume composite and more complex structures tested under tensile load and bending load. The emphasis is on the interplay between fiber orientation, layer arrangement, and matrix–reinforcement interactions on sandwich structures where few reinforced layers alternate with one or more unreinforced layers. The study verifies the applicability of the methodology proposed by Galati et al. (Ref 22) for the tensile behavior to estimate the bending behavior of single-layer reinforced components using a FE model which is calibrated using a minimum number of experimental data points collected with specific fiber orientations. Subsequently, more complex conditions are simulated, and the predictions are compared with results from an extensive experimental campaign.

For the study, three sets of samples are designed and produced: the sandwiched structures which are tested under tensile, the specimens for flexural tests, and the specimens for the model calibration. The sandwiched structures are designed in three configurations: (a) two reinforced layers alternated with one unreinforced matrix layer, (b) two reinforced layers alternated with five unreinforced matrix layers, and (c) three reinforced layers alternated with four unreinforced matrix layers. The orientation of the fiber is alternatively $-45°$ and 45°. The specimens for the bending test are designed to have only one reinforced layer positioned at the center of the specimen and are tested in three-point tests. To identify the effect of the fiber orientation on the flexural properties of the composite material, three configurations are tested: 0°, 45°, and 90°. Additional specimens in pure nylon are used as a reference for the matrix properties and with reinforcing fiber deposited at 60° for numerical model validation. For the model calibration, behind the pure nylon, three configurations of the samples are produced in which the central layer is the only one reinforced with a fiber orientation of 0°, 45°, and 90°, respectively. All specimens are produced with a MarkTwo desktop 3D printer, a CFF system supplied by Markforged. Including the replicas, a total of 60 samples are produced. The paper is organized as follows: Section 2.1 and 2.2 provide a full description of the CFF process patented by Markforged. Section 2.3 details the implementation and calibration of the finite element model used to analyze bending behavior. Section 3 discusses the results, emphasizing the impact of both the number of reinforced layers and the unreinforced (matrix) layers positioned between them. Finally, section 4 concludes the paper and suggests directions for future research.

2. Methods

2.1 CFF Process

The CFF process is an extrusion additive manufacturing patented by Markforged. The system has a print head that contains two nozzles: One nozzle is used to print the matrix material, while the second nozzle is used to deposit the reinforcing fiber. The extrusion head is also equipped with a cutter, which cuts the fiber after the continuous deposition of the reinforcing fiber over the entire area to be reinforced. According to the orientation of the deposited fiber, during the deposition, the fiber is bent to allow the continuous deposition of parallel tracks. In the turning points, the stiffness of the fiber creates a sort of eyelet with missing material. In addition, according to the geometry and the width of the fiber, it is not always possible to deposit the fiber in a continuous manner. In these cases, the void areas are filled locally with the deposition of the matrix. The machine control calculates the deposition path after the selection of the type of reinforcing fiber, the area (or layer) to be reinforced and the deposition angle for the fiber. Figure 1 shows a schematic view of the process with the main hardware.

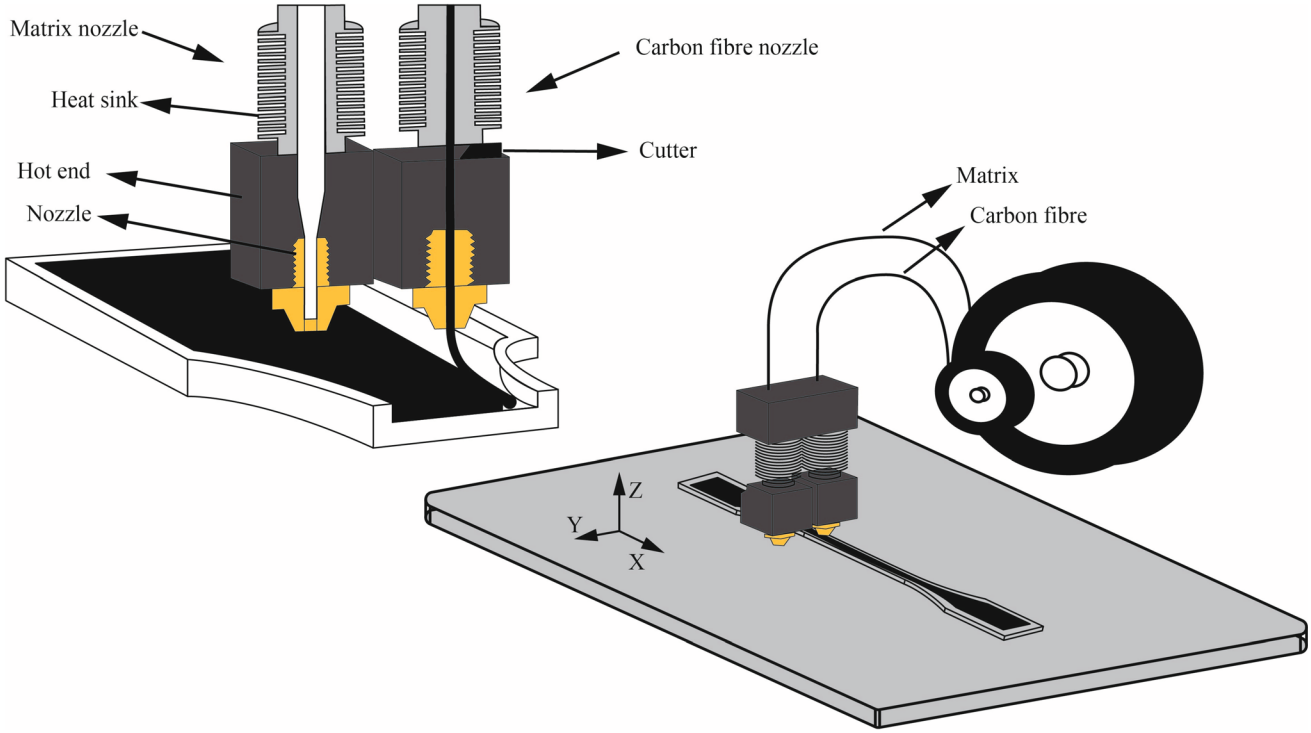


Fig. 1 Schematic view of the process with the main view of the hardware

All the samples used in the study were produced using a MarkTwo desktop 3D printer using standard materials supplied by Markforged. The Cartesian structure of the machine has a build volume of 320 × 132 × 154 mm^3. The matrix was a white nylon-based filament, called Nylon white and supplied by Markforged. Nylon white is a newly developed and stronger nylon matrix with respect to the previous nylon matrix provided by Markforged (Ref 23). The reinforcing filament was carbon (Ref 24). The diameter of the filament was 1.750 mm for the nylon and 0.200 mm for the carbon fiber. The extrusion temperature for the matrix and reinforcing fiber was 275 °C and 230 °C, respectively. The height of the part along the build direction must be a multiple of the layer thickness, which in the case of carbon fiber-reinforced product was equal to 0.125 mm. The extrusion temperatures and the layer thickness are automatically selected by the machine control, Eiger, once the reinforcing fiber is selected. In addition, a minimum of 1 wall for each inner and outer contour of the printed object is required. The infill was selected as "full" for the nylon matrix and isotropic for the fiber to ensure mechanical performance as a function of the orientation of the fiber.

2.2 Design of Specimens and Mechanical Testing

The specimens for the tensile and flexural tests were designed in accordance with ASTM D638 Type II (Ref 25) and ASTM D790 (Ref 26), respectively, as represented in Fig. 2. It should be noted that the width of the tensile specimen has been slightly modified with respect to ASTM D638 Type II because the inner and outer perimeter of each layer needs a minimum of 1 wall to contain the fiber filament.

Imposing a build orientation normal to the largest section of the specimen (z-axis in Fig. 2), the thickness of the specimen has been slightly adapted to accommodate a whole number of layers. Therefore, both specimens count 25 layers. Each layer

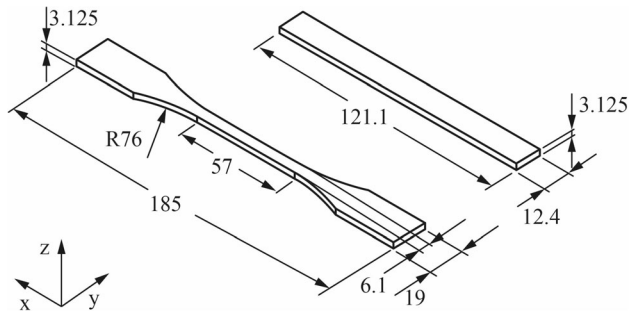


Fig. 2 Geometry and dimensions of the test samples. Measure in mm. z represents the build direction

was numbered from #1 to #25, where layer #1 is attached to the build plate (plane xy in Fig. 2) and layer #13 is the central layer. The geometry was modeled using SolidWorks, exported as an STL file and imported into the machine control software.

The sandwiched structures were designed to have more reinforced layers alternated with matrix layers. The specimen 2L-A was designed with the reinforced layers positioned at layer #12 and layer #14 (Fig. 3a). In other words, considering the central layer as layer 0, layer - 1 and + 1 were reinforced, while the central layer was unreinforced. The specimen 2L-B was designed with the reinforced layers located at layer #10 and layer #16. In other words, considering the central layer as layer 0, the layers − 3 and + 3 were reinforced, while five layers in between (layers − 2, − 1, 0, + 1, and + 2) were unreinforced. The specimen named 3L was designed with three reinforced layers positioned at layer #8, layer #13, and layer #18, respectively (Fig. 3b). In other words, considering the central layer as layer 0, the layers - 5, 0, and + 5, were reinforced, and in between two reinforced layers, there were four

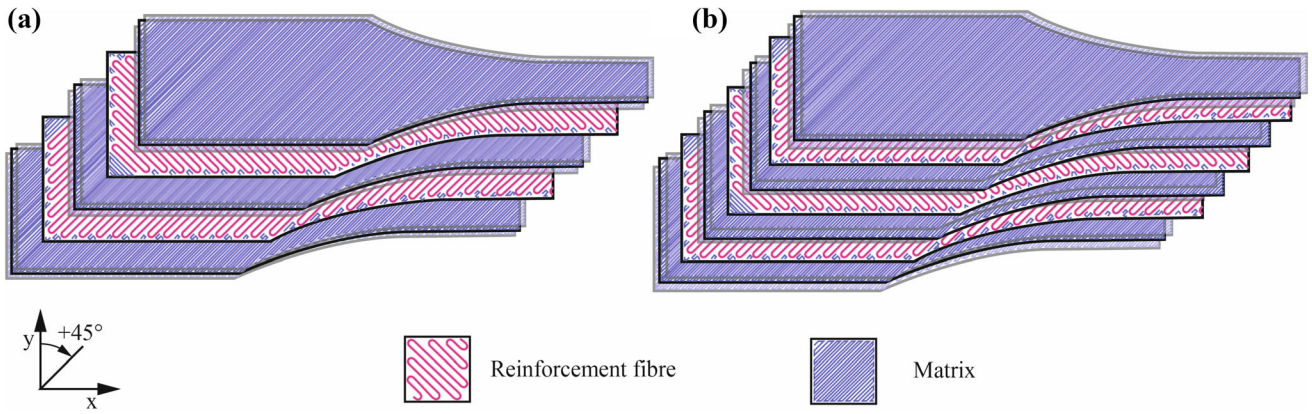


Fig. 3 Schematic representation of the layer distribution inside the sample. (a) Sample with two reinforced layers alternated with one unreinforced layer. (b) Sample with three reinforced layers. Four unreinforced layers are placed between two reinforced layers

unreinforced layers. The orientation of the fiber has been selected alternatively − 45° and 45° as shown in Fig. 3a).

These structures have been tested under a tensile load. The tensile tests were performed using a hydraulic AURA Easydur tensile machine with a maximum load of 10 tons. The samples were tested with a loading rate of 5 mm/min.

Owing to the lack of data on the bending properties, the specimens for the bending test have been designed to have only one reinforced layer positioned at the center of the specimen (layer #13). To identify the effect of the fiber orientation on the flexural properties of the composite material, three configurations have been tested: 0°, 45°, and 90°. Additional specimens were produced in pure nylon, a specimen as a reference for the matrix properties, and a specimen with reinforcing fiber deposited at 60° for material validation. The bending test was performed on a hydraulic AURA Easydur machine for the three-point test (Fig. 4) with a maximum load of 5 tons. The speed of the crosshead was set at 1.4 mm/min, while the span was set to 50 mm according to the standard (Ref 26). After a preliminary test in which the specimen never reached the breaking point, a maximum stroke of 15 mm has been set.

For each design, five replicas have been manufactured and tested. All samples were tested within a maximum of 12 hours from production to avoid the detrimental effects of the absorption of air moisture from the nylon matrix.

2.3 Finite Element Analysis

The FE model was developed according to the methodology proposed by Galati et al. (Ref 22). Owing to the anisotropic behavior of the composite material, the material properties must be calibrated by determining the longitudinal elastic modulus E_1, the transverse elastic modulus E_2, and the in-plane shear modulus G_{12} to be assigned to the reinforced layer. With this scope, additional specimens reinforced with carbon fiber have been printed according to the geometry in Fig. 2, in which only the central layer (layer #13) has been reinforced. To obtain the corresponding properties, the reinforcing fiber has been deposited along the tensile load direction (0°) to determine E_1 and at 90° and 45° to establish E_2 and G_{12}, respectively. An additional sample using only nylon has been manufactured and tested to determine the material properties of the matrix. In this case, the nylon has been assumed to be isotropic. Furthermore, the FE model was verified using an additional sample in which the central layer was reinforced with a reinforcing fiber deposited at 60°. This configuration establishes an example of the anisotropic behavior of the composite material. For each configuration, five replicas have been manufactured, for a total of 25 samples.

The model was implemented and solved using Hyperworks and Optistruct. The discretization of the domain has been performed using 3D Hexa mesh with 1 mm of maximum element size, while the thickness of the element was defined according to the layer thickness equal to 0.125 mm. The model includes 25 layers, corresponding to the number of layers printed for the sample. Each layer bonded to the adjacent ones to obtain displacement consistency. According to the tested condition, the reinforced layer (or layers) is modeled differently to account for the nylon matrix in the perimeter surrounding the reinforcement fiber. The nylon is simulated as an isotropic and homogenous material, while the reinforced layer (RF) is simulated as a homogenous and orthotropic material. To account for the fiber deposition orientation, a local material system is applied to each element of the RF area. For each simulation, the local material system is rotated according to the fiber orientation. The first axis of the local system is oriented along the deposition direction, the second axis is perpendicular to the deposition direction, and the third axis is perpendicular to the deposition plane.

The setup of the model for the tensile test is resumed in Figure 5, in which the constraint and the load emulate the tensile test. The material properties of the reinforced layer were tuned according to the experimental results and the corresponding fiber orientation. The procedure for the material properties tuning is reported in the flowchart in Figure 6. More details on the modeling and model calibration can be found in (Ref 27).

After the material properties tuning, the model has been tested under several conditions by adapting the modeling setup correspondingly: (a) reinforced sample with the fiber orientation at 60° under tensile load; (b) sandwiched structures with different quantities, locations, and orientations of the fiber-reinforced layers under tensile load; and (c) bending conditions under different orientations of the fiber-reinforced layer. While the model tested under tensile load was only varied according to the corresponding specimen design, the model setup for the bending test is represented in Fig. 7. The mesh characteristics were kept the same as that for the tensile simulation.

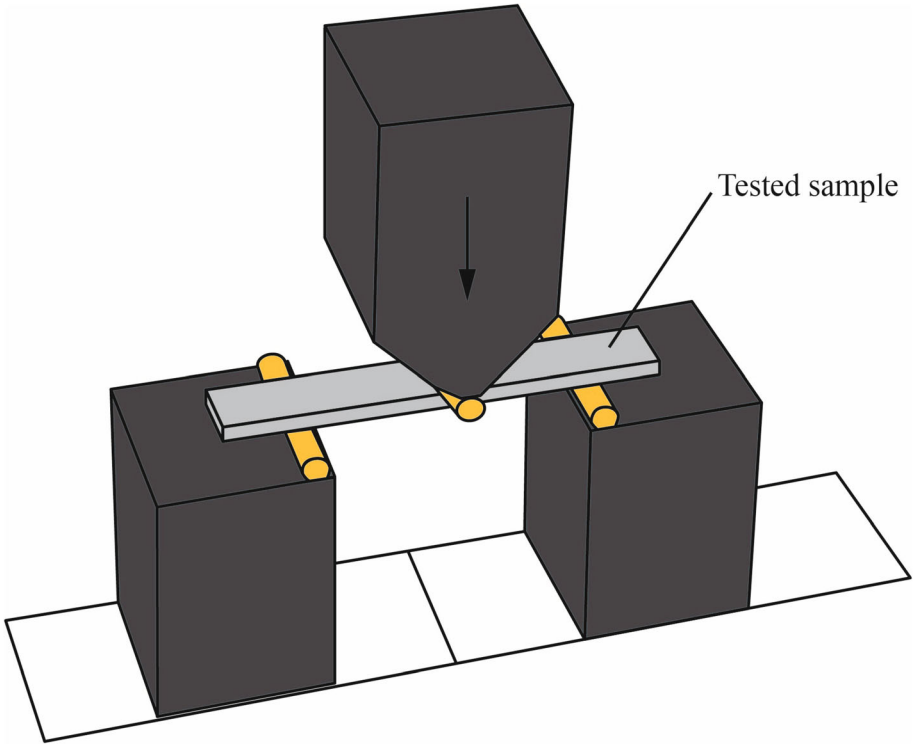


Fig. 4 Schematic representation of the 3 points flexural test

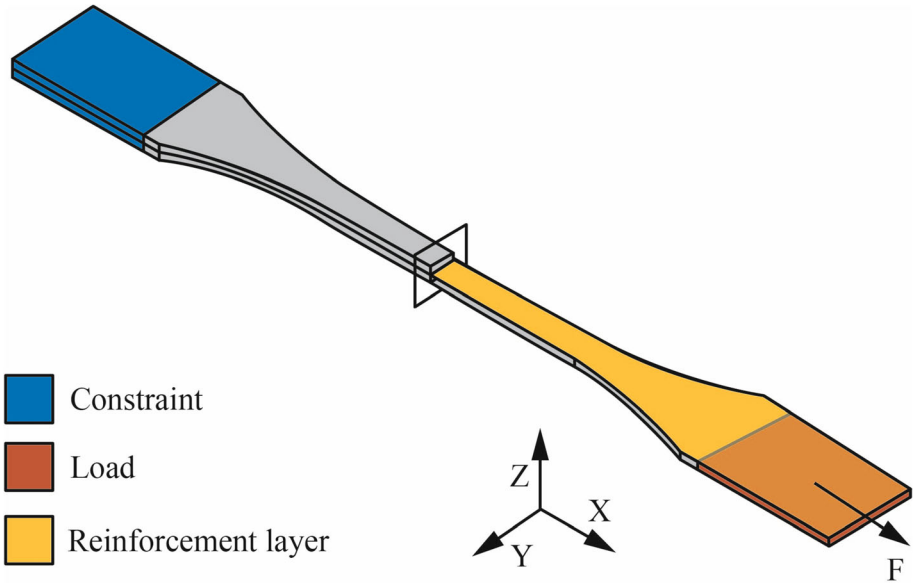


Fig. 5 Model setup for FE analysis of tensile test

3. Summary of the Produced Specimen

Table 1 resumes the characteristics of the reinforced designed specimen, the testing, and the objective. In addition, the quantity of material in terms of filament length used to produce each specimen in that specific configuration is reported. The fiber ratio describes the quantity of total fiber with respect to the matrix material and highlights the limited fiber quantity. Those data have been extracted from the machine control software Eiger. Table 1 does not report the specimens in pure nylon.

4. Results and Discussion

4.1 Tensile Tests

Figure 8 compares the designed deposition path (on the right) with the actual manufactured deposited one (on the left) in the correspondence of the central layer. Each sample was identified by "CF" (carbon fiber) followed by the angle fiber orientation. As can be observed, the fiber is deposited in a continuous manner. However, the presence of turning points creates an area (similar to an eyelet) in which the fiber is

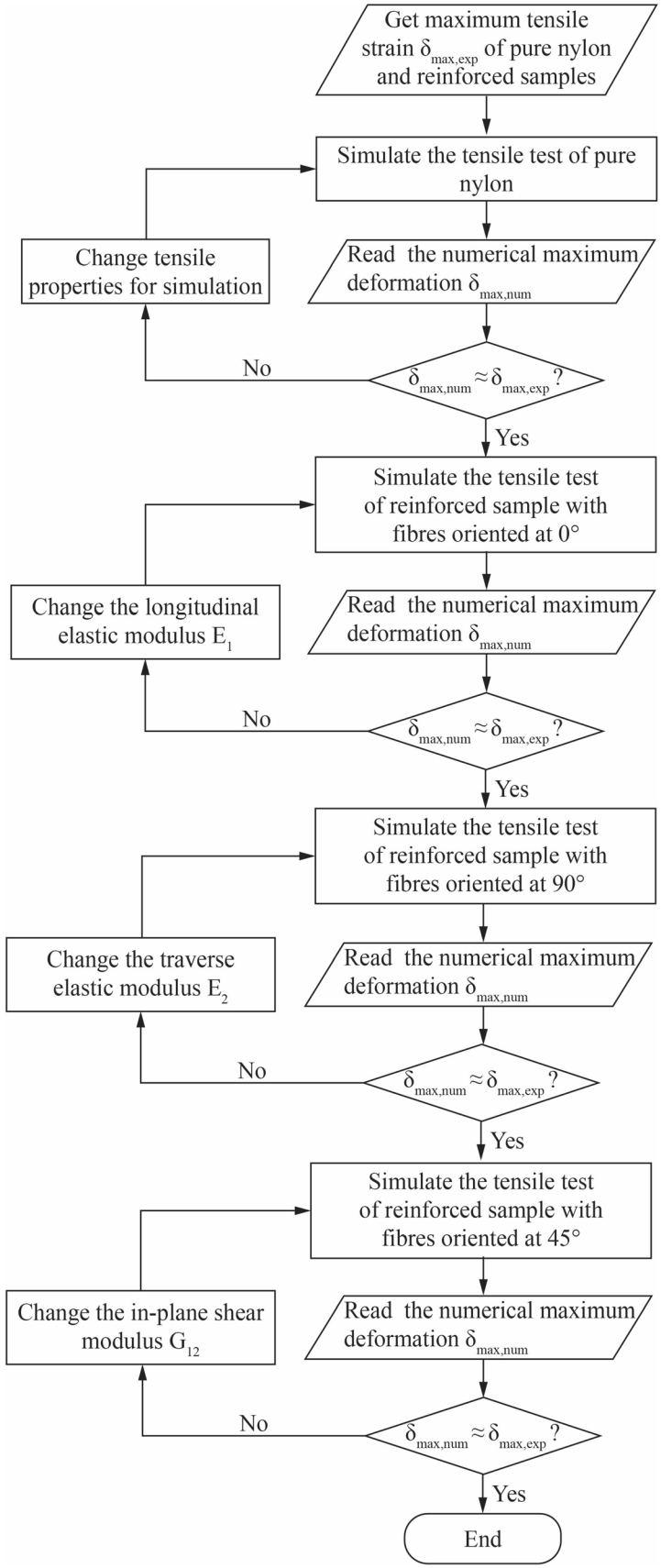


Fig. 6 Flowchart of the tuning of the material properties for FE analysis. Adapted from Galati et al. (Ref 22)

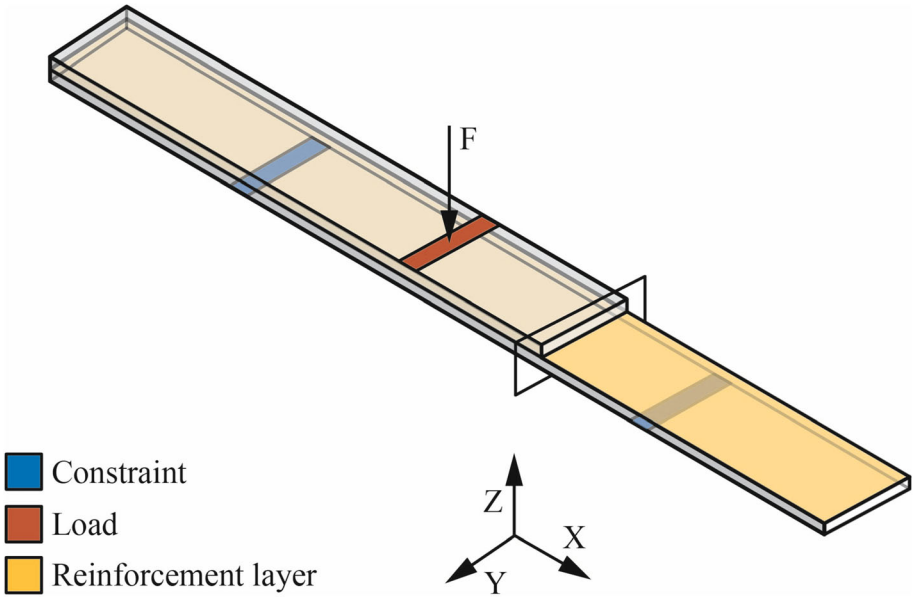


Fig. 7 Model setup for FE analysis of bending test

Table 1 Characteristics of the produced specimen. The position of the reinforced layer is provided considering the central layer of the specimen as layer 0

Index	Testing	Number of reinforced layer and position of the reinforced layer	Fiber orientation	Objective	Nylon, mm^3	Carbon fiber, mm^3	Fiber ratio, %
CF0	Tensile	One layer layer 0	0°	Model calibration	6390	220	3.3
CF90	Tensile	One layer layer 0	90°	Model calibration	6380	220	3.3
CF45	Tensile	One layer layer 0	45°	Model calibration	6390	220	3.3
CF60	Tensile	One layer layer 0	60°	Model validation	6380	220	3.3
2L-A	Tensile	Two layers layer + 1 and layer − 1	45 and − 45°	Characterization and model validation	6170	430	6.5
2L-B	Tensile	Two layers, layer + 3 and layer − 3	45 and − 45°	Characterization and model validation	6180	430	6.5
3L	Tensile	Three layers layer + 5, layer 0 and layer − 3	45 and − 45°	Characterization and model validation	6030	650	9.7
CF0	Bending	One layer layer 0	0°	Characterization and model validation	4300	140	3.1
CF90	Bending	One layer layer 0	90°	Characterization and model validation	4270	140	3.2
CF45	Bending	One layer layer 0	45°	Characterization and model validation	4280	140	3.1

missing. This aspect of the component is peculiar to the AM process and makes crucial the analysis of the process-dependent material properties.

Table 2 reports the relative values and the standard deviation calculator of the five replicas for the single-layer reinforced sample in terms of Young's modulus (E) and ultimate strain (ε_{ult}). As can be observed, the highest Young's modulus was registered when the fiber was orientated parallel to the load direction (CF0). On the contrary, the maximum elongation is measured for the fiber deposited perpendicular to the load direction (CF 90). In this direction, the matrix properties contribute the most. For intermediated orientation, while Young's modulus is significantly lower than CF0, the elongation is comparable to CF45. As demonstrated by the low standard deviation, the process shows a high repeatability.

Figure 9 shows the force–displacement curve averaged on the five replicas of the tensile test as a function of the deposition orientation of the fiber. For comparison, the curves corresponding to the sandwiched structures have also been reported. As expected, even the introduction of the reinforcement in a single layer improves the properties of the material compared to pure nylon. The orientation of the fiber has a strong influence on the

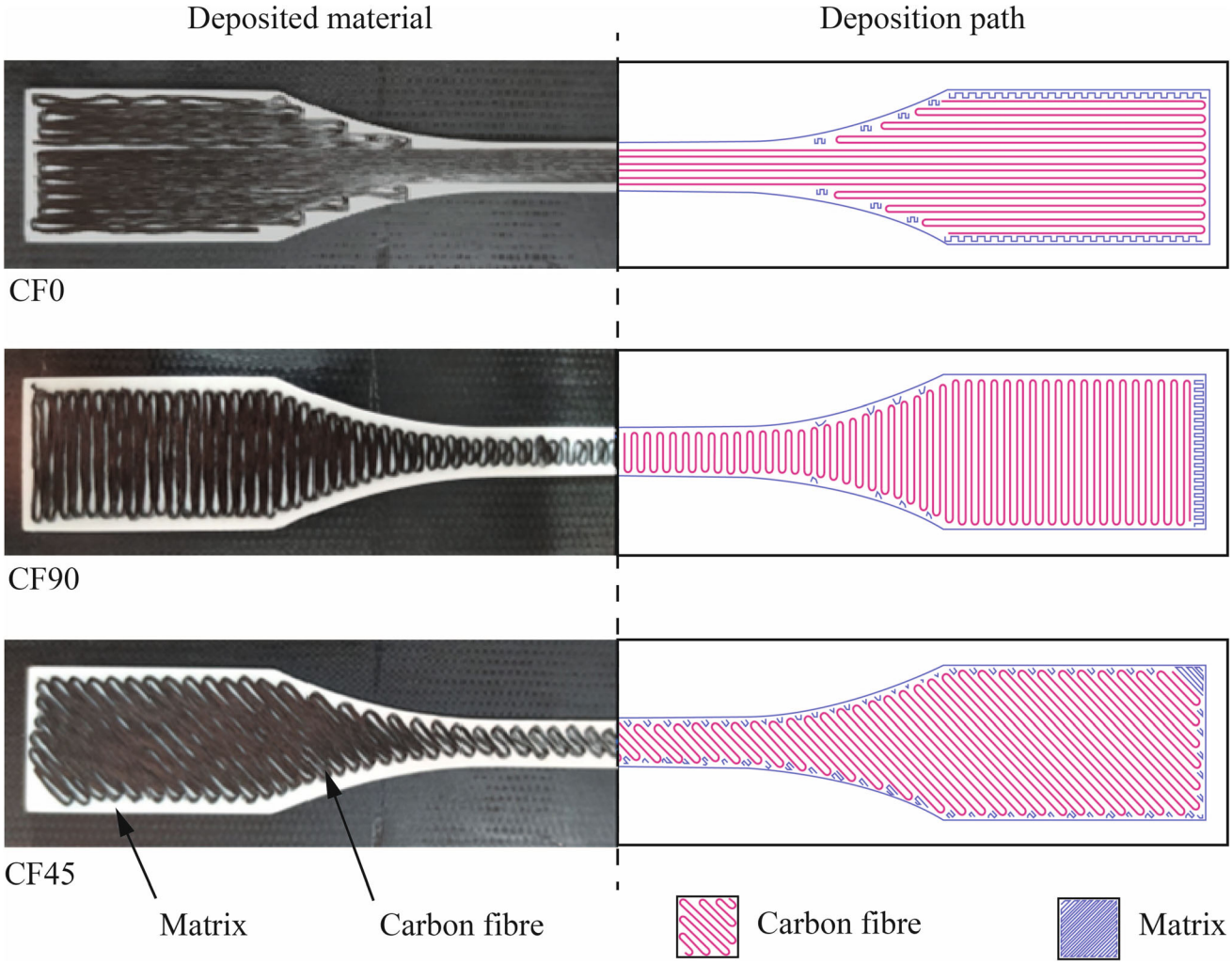


Fig. 8 Comparison of deposited material (left) and designed deposition path (right)

Table 2 Mechanical properties for the single-layer reinforced specimen

Sample	E, MPa	$\varepsilon_{ult,\ \%}$
CF0	1435 ± 64	4.5 ± 1.0
CF90	695 ± 16	35 ± 9.0
CF45	705 ± 10	26.9 ± 6.9
CF60	652 ± 52	33.7 ± 3.3

material properties. The highest properties with the highest values of strength correspond to the sample's 90° reinforced fiber, which, on the other hand, showed a brittle failure. This is explained by the fact that the fiber is aligned with the load direction (Ref 15). As the orientation deposition angle increases for the sample reinforced in one single layer, the slope of the curve is reduced. However, no significant difference can be observed among the samples. Comparing the sandwiched samples to the single layer deposited at 45°, it is possible to notice that not only the quantity of the reinforced layer influences the mechanical properties, but also the location of the reinforced layers. In particular, the quantity of reinforced layer appears to influence the mechanical strength while the location influences the maximum deformation. When the number of matrix layers between two reinforced layers increases, the elongation also increases (2L-A vs 2L-B). When the number of reinforced layers increases, the strength (yield point) also increases, while the maximum elongation is only slightly reduced. This can be explained by the fact that when reinforced layers are closely spaced, they interact with each other in a way that collectively enhances the sample's performance. However, as the number of matrix layers between two reinforced layers increases, the behavior of the matrix becomes more dominant, and the distance between the reinforced layers becomes too great to maintain sufficient stiffness, leading to increased elongation of the matrix.

4.2 Bending Test

Figure 10 shows the designed path compared to the deposited one for each configuration. As can be observed, the fiber is deposited in a continuous manner. The central part of the sample CF0 is uniform along the longest edge. In this area, the fiber can be deposited without interruptions or sudden path modifications, which may create discontinuities in the deposition. As already observed for the tensile specimens, these discontinuities can be detected at the turning points of the deposition path, which create localized voids.

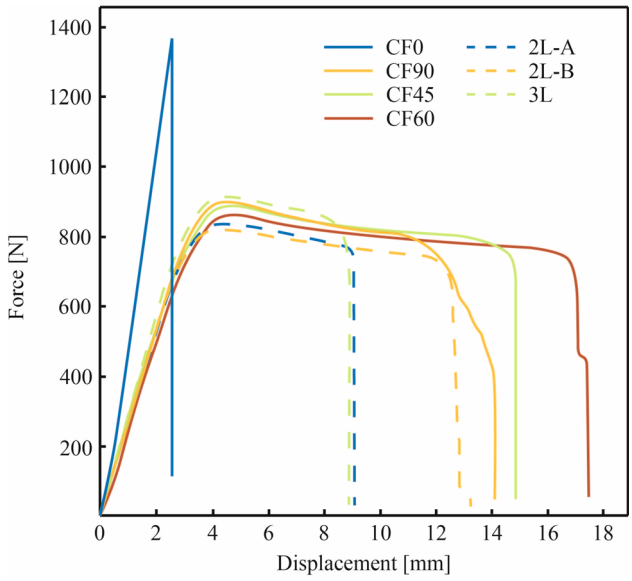


Fig. 9 Solid lines represent the average force–displacement curve for the different orientations of the carbon fiber. Dashed lines represent the force–displacement curves for the sandwiched structures. The samples reinforced with a single layer are named using "CF" which stands for carbon fiber, followed by the angle orientation of the fiber

Figure 11 shows the average curve of force–displacement among the five replicas for each configuration. No significant differences can be noticed for the different orientations of the deposited fiber in the initial response of the material elastic zone. The same finding can be found by observing the average value of chord modulus at different fiber orientations in Table 3. By increasing the deformation, a slight difference can be noted for the specimen reinforced with the fiber deposited at 90° reinforcement. For these samples, the resistance is lower because the fiber does not offer any resistance to the bending, which is only accommodated by the deposition path. Particularly, by increasing the deformation, it appears that the matrix characteristics become predominant, reaching the performance of pure nylon (No CF in Fig. 11). This can be explained by the orientation of the fiber with respect to the bending load. In fact, the specimens in which the fiber is oriented with a different angle show a significant difference with respect to the unreinforced specimen. In this case, the fiber is able to counteract the bending load. When the fiber is oriented differently from 90°, the strength is about 25% higher.

4.3 FE Analysis and Validation

As mentioned above, the results from the samples in pure nylon and with the single reinforced layer at 0°, 45°, and 90° have been used to calibrate the material properties of the matrix

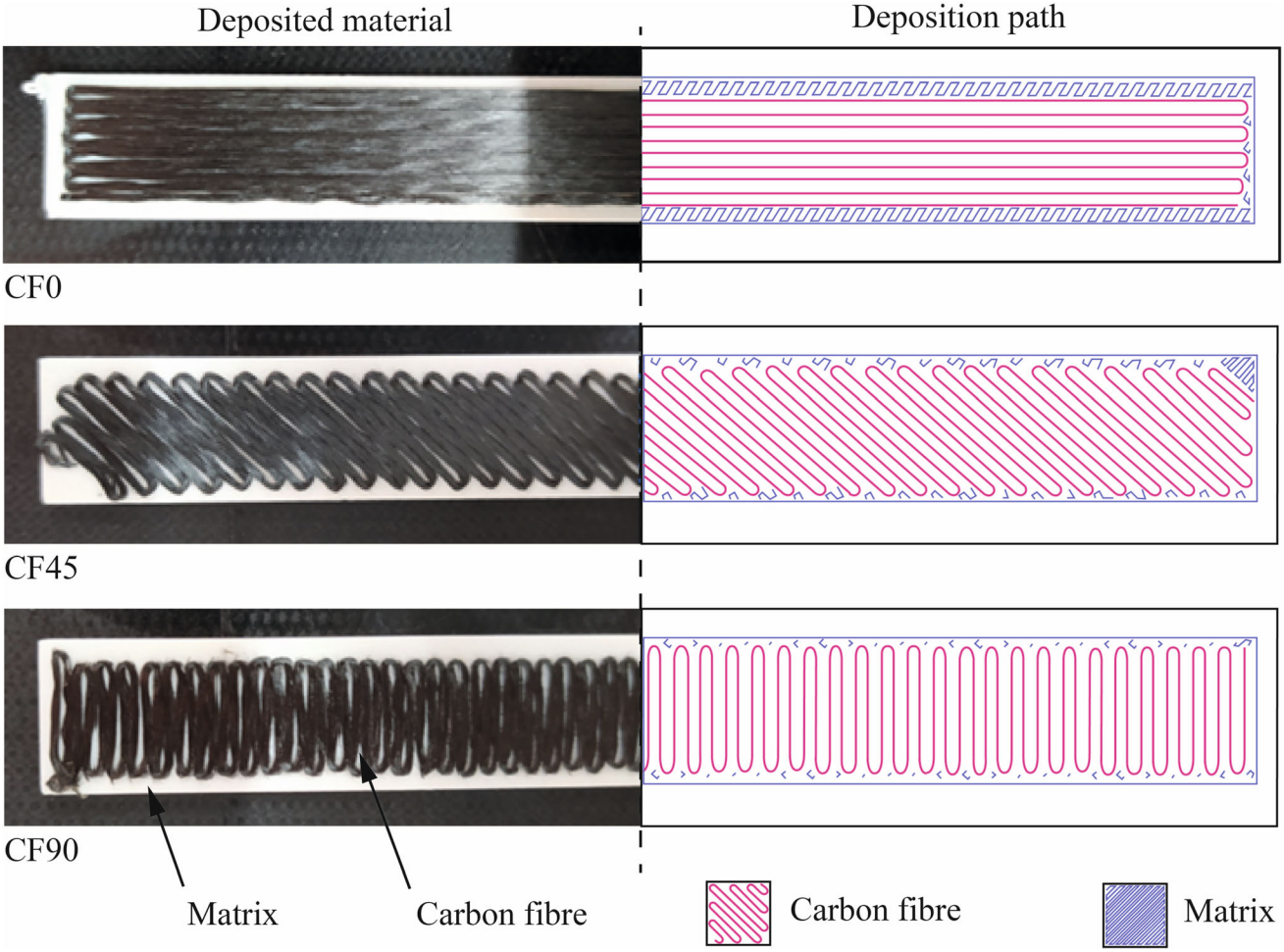


Fig. 10 Deposited material (left) and designed deposition path (right)

and the reinforcing fiber, respectively, of the FE model. According to the proposed approach, initially, the pure nylon specimens printed at different layer thicknesses have been simulated. As the first attempt, the mechanical properties of the nylon and reinforcing fiber are extracted from the Markforged datasheet (Ref 28) and reported in Table 4. These datasheet values are the results of the tests made by Markforged Inc. according to ASTM D638 for the nylon and ASTM D3039 for the fiber without additional specifications. To calibrate the material properties of the nylon in the FE model, the material properties are changed step by step until the convergence between numerical and experimental results, according to the procedure reported in Fig. 6. The obtained results are summarized in Table 4. As can be observed, the corresponding properties are significantly different from the data supplied by Markforged. This can be explained by the fact that the process-induced defects, such as the absence of reinforced fiber at the turning points (as an example, see Fig. 8), significantly influence the material response. Those defects induce a weaker response of the material. To account for such an effect, the material model implemented the values obtained from the experimental campaign.

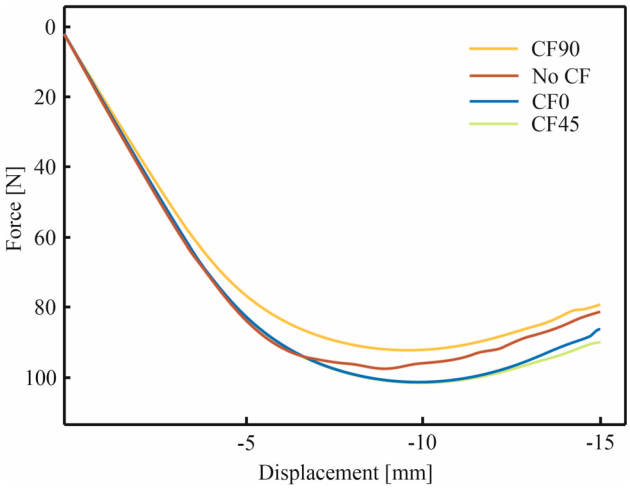


Fig. 11 The average force–displacement curve for the different fiber orientations configuration

Table 3 Chord modulus at different fiber orientations with the corresponding standard deviation calculated over the five tested replicas

Sample	E_f, MPa
CF0	1423 ± 70
CF90	1330 ± 85
CF45	1423 ± 170

For validation purposes, the numerical force–displacement curve is computed under different conditions and compared with the corresponding experimental following cases: (a) specimen with a single reinforced layer with the fiber deposited at 60° and tested under tensile load; (b) sandwiched structures under tensile load; (c) specimens reinforced in a single layer at different fiber orientations and tested under a bending load.

Under tensile loads, the model's response was in agreement with the experimental results. Figure 12 shows a comparison between the numerical and experimental results in terms of displacement measured (or estimated) at 500 N. As observed, the deviation between experimental and predicted displacements is always below 13%, which falls within the experimental standard deviation due to process-induced defects (Fig. 12).

The maximum deviation is observed when only a single layer is reinforced, as voids in the layer play a major role. However, the deviation is reduced to 1% (2L-A) when the number of reinforced layers increases, especially when the fiber is deposited in subsequent layers perpendicular to the previous fiber orientation. This configuration allows a better load distribution within the fiber and reduces the impact of fiber vacancies. This finding aligns with the deviation observed for the 3L sample, where the even number of layers exhibits a similar effect to that observed in the single reinforced layer. Nevertheless, the predicted displacement remains within the experimental deviation.

As far as the validation of the model under a bending load, the tests confirmed the excellent capability of the model in predicting the mechanical behavior of the material. In this case, the deviation from the experimental results is always lower than 2%, and it can also capture the limited fiber orientations to the bending behavior (displacement almost independent of the orientation). Figure 13 shows an example corresponding to a force equal to 30 N. The deviation is constant, meaning the presence of a systematic error in the numerical model, which also, in this case, could be attributed to the material modeling.

5. Conclusion

This study provides a comprehensive analysis of the mechanical properties of composite materials produced by additive manufacturing (AM) with continuous fiber reinforcement (CFF). Unlike traditional methods that use plies, AM with

Table 4 Material model properties for the FE model compared to the data from the supplier

			Datasheet from the supplier	Material model
Nylon	E	[MPa]	1700	1481
	G	[MPa]	611	532
	v		0.39	0.39
Fiber	E_1	[MPa]	60000	40000
	E_2	[MPa]	7500	1000
	$v_{12} = v$		0.15	0.15
	G_{12}	[MPa]	4000	25

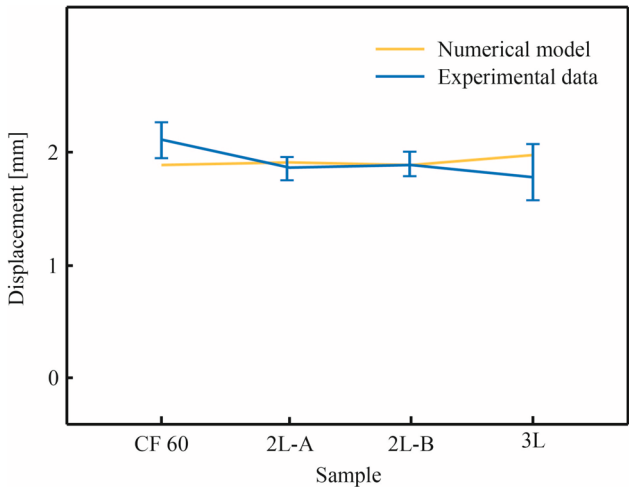


Fig. 12 Comparison of the experimental displacement with the displacement obtained numerically for the different samples at 500 N

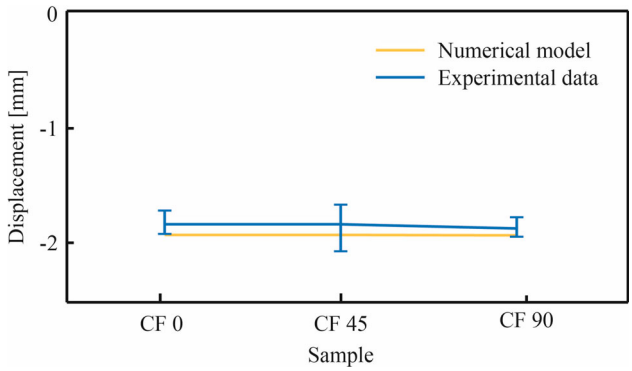


Fig. 13 Comparison of experimental and numerical data in the case of a load of 30 N

CFF involves depositing reinforcing fibers continuously along a predefined path, necessitating directional modifications at turning points to ensure complete area reinforcement. These modifications create local variations in material properties, particularly at fiber eyelets.

The research focused on characterizing the tensile and flexural behavior of a composite material comprising a nylon matrix and carbon fiber reinforcement, including sandwich structures. A finite element (FE) model was developed to capture the unique aspects of the AM process, which was validated against experimental data. Key findings include:

1. Tensile behavior:
- As excepted, fibers aligned with the load direction provided the highest resistance and exhibited brittle fracture. Young's modulus significantly decreased with varying fiber orientations from 90°, even for sandwich structures. However, for orientations different from 90°, the variation among samples is minimal.
- Multiple reinforced layers influenced yield points and elongation. However, contrary to expectations these mechanical properties are influenced not only by the number of reinforced layers but also by the number of unreinforced layers between two reinforced ones. Increased unreinforced layers between reinforced layers enhanced elongation, suggesting that layer number and positioning are crucial design parameters.

2. Flexural behavior:
- Different fiber orientations did not significantly improve performance compared to unreinforced samples in the elastic region.
- In the plastic region, fibers oriented at 90° offered the best resistance.

The FE model effectively predicted the mechanical behavior under both tensile and bending loads, showing negligible deviation from experimental results. This model proved capable of accurately estimating the effects of fiber deposition, even with multiple reinforced layers.

This study also highlights the potential of producing matrix-dominant composites with low fiber volume fractions using AM with CFF. By focusing on sustainability, these materials can reduce the environmental impact of traditional composites, which are often challenging to recycle due to their high fiber content and complex architecture. The ability to tailor reinforcement placement and fiber volume enables the design of lightweight, durable, and recyclable composites suitable for applications typically not considered for composites, such as wearable devices and other consumer products. The validated finite element (FE) model presented herein serves as a robust preliminary predictive tool, facilitating the design of more complex AM components. Additionally, the study reveals the significant impact of the position, number of reinforced layers, and the matrix layer interposition on material properties. This underscores the need for further experimental data to complement the FE model, ultimately optimizing the development of advanced composite materials for diverse engineering.

Acknowledgments

Financed by the European Union—NextGenerationEU (National Sustainable Mobility Center CN00000023, Italian Ministry of University and Research Decree n. 1033—17/06/2022, Spoke 11—Innovative Materials & Lightweighting). The opinions expressed are those of the authors only and should not be considered as representative of the European Union or the European Commission's official position. Neither the European Union nor the European Commission can be held responsible for them.

Author contributions

Manuela Galati contributed to conceptualization, data curation, formal analysis, methodology, project administration, validation, and writing—original draft. Paolo Minetola contributed to conceptualization, methodology, and writing—review and editing. Giovanni Rizza contributed to data curation, visualization, and writing—review and editing.

Funding

Open access funding provided by Politecnico di Torino within the CRUI-CARE Agreement.

Open Access

This article is licensed under a Creative Commons Attribution 4.0 International License, which permits use, sharing, adaptation, distribution and reproduction in any medium or format, as long as you give appropriate credit to the original author(s) and the source, provide a link to the Creative Commons licence, and indicate if changes were made. The images or other third party material in this article are included in the article's Creative Commons licence, unless indicated otherwise in a credit line to the material. If material is not included in the article's Creative Commons licence and your intended use is not permitted by statutory regulation or exceeds the permitted use, you will need to obtain permission directly from the copyright holder. To view a copy of this licence, visit http://creativecommons.org/licenses/by/4.0/.

References

1. D. Ukobitz and R. Faullant, Leveraging 3D Printing Technologies: The Case of Mexico's Footwear Industry, *Res.-Technol. Manag.*, 2021, **64**(2), p 20–30.
2. J.M. Pearce, Return on Investment for Open Source Scientific Hardware Development, *Sci. Public Policy*, 2016, **43**(2), p 192–195.
3. P. Tack, J. Victor, P. Gemmel, and L. Annemans, 3D-Printing Techniques in a Medical Setting: A Systematic Literature Review, *BioMed. Eng. Online*, 2016, **2016**, p 1–21.
4. W. Jamróz, J. Szafraniec, M. Kurek, and R. Jachowicz, 3D printing in Pharmaceutical and Medical Applications—Recent Achievements and Challenges, *Pharm. Res.*, 2018, **35**(9), p 176.
5. S.C. Joshi and A.A. Sheikh, 3D Printing in Aerospace and Its Long-Term Sustainability, *Virtual Phys. Prototyp.*, 2015, **10**(4), p 175–185.
6. 3D Systems to Develop 3D Printing for US Aerospace and Defense, *Met. Powder Rep.*, **70**(3), p 152–153
7. M.R. Nichols, How Does the Automotive Industry Benefit from 3D Metal Printing?, *Met. Powder Rep.*, 2019, **74**(5), p 257–258.
8. B.A. Moreno-Núñez, M.A. Guerrero-Alvarado, A. Salgado-Castillo, C.D. Treviño-Quintanilla, E. Cuan-Urquizo, U. Sánchez-Santana, and G. Pincheira-Orellana, Build and Raster Orientation Effects on CFRP Onyx/Aramid Impact Absorption, *Compos. Part C Open Access*, 2024, **14**, 100485
9. A. Vedrtnam, P. Ghabezi, D. Gunwant, Y. Jiang, O. Sam-Daliri, N. Harrison, J. Goggins, and W. Finnegan, Mechanical Performance of 3D-Printed Continuous Fibre Onyx Composites for Drone Applications: An Experimental and Numerical Analysis, *Compos. Part C: Open Access*, 2023, **12**, 100418
10. C. Pandelidi, S. Bateman, S. Piegert, R. Hoehner, I. Kelbassa, and M. Brandt, The Technology of Continuous Fibre-Reinforced Polymers: A Review on Extrusion Additive Manufacturing Methods, *Int. J. Adv. Manuf. Technol.*, 2021, **113**(11), p 3057–3077.
11. G.W. Melenka, B.K.O. Cheung, J.S. Schofield, M.R. Dawson, and J.P. Carey, Evaluation and Prediction of the Tensile Properties of Continuous Fiber-Reinforced 3D Printed Structures, *Compos. Struct.*, 2016, **153**, p 866–875.
12. F. Van Der Klift, Y. Koga, A. Todoroki, M. Ueda, Y. Hirano, and R. Matsuzaki, 3D Printing of Continuous Carbon Fibre Reinforced Thermo-Plastic (CFRTP) Tensile Test Specimens, *Open J. Compos. Mater.*, 2016, **06**(01), p 18–27.
13. M.N. Islam, K.P. Baxevanakis, and V.V. Silberschmidt, Viscoelastic Characterisation of Additively Manufactured Composites with Nylon Matrix: Effects of Type and Orientation of Fibres, *Compos. Part B Eng.*, 2023, **263**, 110815
14. A.N. Dickson, J.N. Barry, K.A. McDonnell, and D.P. Dowling, Fabrication of Continuous Carbon, Glass and Kevlar Fibre Reinforced Polymer Composites Using Additive Manufacturing, *Addit. Manuf.*, 2017, **16**, p 146–152.
15. J. Justo, L. Távara, L. García-Guzmán, and F. París, Characterization of 3D Printed Long Fibre Reinforced Composites, *Compos. Struct.*, 2018, **185**, p 537–548.
16. S. Sangaletti, M.T. Aranda, L. Távara, and I.G. García, Effect of Stacking Direction and Raster Angle on the Fracture Properties of Onyx 3D Printed Components: A Mesoscale Analysis, *Theor. Appl. Fract. Mech.*, 2024, **129**, 104228
17. V. Lunetto, M. Galati, L. Settineri, and L. Iuliano, Sustainability in the Manufacturing of Composite Materials: A Literature Review and Directions for Future Research, *J. Manuf. Process.*, 2023, **85**, p 858–874.
18. J. Luo, K. Zou, Q. Luo, Q. Li, and G. Sun, On Asymmetric Failure in Additively Manufactured Continuous Carbon Fiber Reinforced Composites, *Compos. Part B Eng.*, 2024, **284**, 111605
19. M. Araya-Calvo, I. López-Gómez, N. Chamberlain-Simon, J.L. León-Salazar, T. Guillén-Girón, J.S. Corrales-Cordero, and O. Sánchez-Brenes, Evaluation of Compressive and Flexural Properties of Continuous Fiber Fabrication Additive Manufacturing Technology, *Addit. Manuf.*, 2018, **22**, p 157–164.
20. J.M. Chacón, M.A. Caminero, P.J. Núñez, E. García-Plaza, I. García-Moreno, and J.M. Reverte, Additive Manufacturing of Continuous Fibre Reinforced Thermoplastic Composites Using Fused Deposition Modelling: Effect of Process Parameters on Mechanical Properties, *Compos. Sci. Technol.*, 2019, **181**, p 107688.
21. H. Al Abadi, H.T. Thai, V. Paton-Cole, and V.I. Patel, Elastic Properties of 3D Printed Fibre-Reinforced Structures, *Compos. Struct.*, 2018, **193**, p 8–18.
22. M. Galati, M. Viccica, and P. Minetola, A Finite Element Approach for the Prediction of the Mechanical Behaviour of Layered Composites Produced by Continuous Filament Fabrication (CFF), *Polym. Test.*, 2021 https://doi.org/10.1016/j.polymertesting.2021.107181
23. "Thermoplastic 3D Printing Material - Nylon White," n.d., https://markforged.com/materials/plastics/nylon. Accessed 21 January 2025
24. Markforged, Composite 3D Properties, 2020, p 0–1
25. "Standard Test Method for Tensile Properties of Plastics," 2022
26. Astm International, Standard Test Methods for Flexural Properties of Unreinforced and Reinforced Plastics and Electrical Insulating Materials. D790, *Annu. Book ASTM Stand.*, 2002, p 1–12
27. M. Galati, M. Viccica, and P. Minetola, A Finite Element Approach for the Prediction of the Mechanical Behaviour of Layered Composites Produced by Continuous Filament Fabrication (CFF), *Polym. Test.*, 2021, **98**, 107181
28. "Nylon White Datasheet," 2025, https://web-objects.markforged.com/craft/materials/CompositesV5.2.pdf. Accessed 21 January 2025

Publisher's Note Springer Nature remains neutral with regard to jurisdictional claims in published maps and institutional affiliations.